

**WIND INDUCED VARIABILITY OF HYDROGRAPHIC FEATURES  
AND WATER MASSES DISTRIBUTION IN THE GULF OF CADIZ  
(SW IBERIA) FROM *IN SITU* DATA**

***F. Criado-Aldeanueva<sup>(a)</sup>, J. García-Lafuente<sup>(a)</sup>, J.M. Vargas<sup>(a)</sup>,  
J. Del Río<sup>(a)</sup>, A. Sánchez<sup>(a)</sup>, J. Delgado<sup>(a)</sup> and J.C. Sánchez<sup>(a)</sup>***

<sup>(a)</sup> *Departamento de Física Aplicada II, Universidad de Málaga, Málaga, Spain.*

Corresponding author:

*Francisco Criado Aldeanueva  
Dpto. Física Aplicada II, E.T.S.I. Informática  
Campus de Teatinos, Universidad de Málaga  
29071 Málaga, Spain*

*Tel.: +34 952 132849, Fax: +34 952 131450  
fcaldeanueva@ctima.uma.es*

**ABSTRACT:** In May-June 2001, the GOLFO 2001 survey was carried out in the Gulf of Cadiz area (South-West Iberia). The survey consisted of three legs that were accomplished under different wind regimes. In Mesoscale 1 (under westerlies) North Atlantic Central Water was located in the northern region and Surface Atlantic Water in the outer part and this distribution maintained for the entire upper water column, with the only exception of some traces of Shelf Water in the surface layer closest to the Guadalquivir river mouth. In Mesoscale 2 (under easterlies), Shelf Water was advected westwards by the coastal countercurrent that developed under this regime, thus flooding the surface layer of the eastern (and partly the western) continental shelf and restricting the upwelled North Atlantic Central Water to a smaller region west of 8°W. This pattern only affects the upper 20-25m of the water column, then recovering the common distribution with North Atlantic Central Water in the northern area and Surface Atlantic Water in the outer part of the basin. The wind induced variability modified the surface TS diagrams and these variations have been used to further investigate the water masses distribution in terms of the TS properties of three “standard” points defined on the TS diagram.

**Keywords:** Wind-driven circulation, Meteorological forcing, Water Masses, TS Diagrams, Surface Layer, Gulf of Cadiz (South-West Iberia).

## 1. INTRODUCTION

The Gulf of Cadiz is the sub-basin of the North Atlantic that connects the Atlantic Ocean and the Mediterranean Sea through the Strait of Gibraltar. The most outstanding geographical features are Cape St Maria (CSM), Cape St Vincent (CSV) and Cape Trafalgar, CT (see Figure 1 upper). CSM divides the continental shelf into two halves. To the east of the Cape, the continental shelf is wide (some 30-50 km) and has a gentle slope, whereas to the west it is narrow (< 15 km) and its bottom is dotted with submarine canyons -Faro, Lagos, Portimao, St Vincent- (see Figure 1 upper, again).

--- Approximate location of Figure 1 ---

The main part of the studies carried out in the Gulf of Cadiz have focused on the Mediterranean Water outflow through the Strait of Gibraltar (Zenk, 1970; Bryden and Stommel, 1982; Zenk and Armi, 1990; Ochoa and Bray, 1991; Baringer and Price, 1999; Ambar et al., 2002) and its subsequent mixing with Atlantic waters. Moreover, the formation of *eddies* of Mediterranean origin, the so-called *meddies*, has also been matter of special interest (Serra and Ambar, 2002). The surface circulation of the Gulf of Cadiz is integrated into the general circulation of the Northeast Atlantic: the Azores current, which transports some 15 Sv between latitudes 35°N-40°N to feed the Canary Current, frequently forms meanders that separate themselves from the main flow (Alves et al., 2002). The surface circulation of the Gulf of Cadiz could be understood as the last meander of the Azores current that, as entering through the Strait of Gibraltar, counters the outflow of Mediterranean Water.

Most of the studies on the surface circulation deal with remotely sensed Sea Surface Temperature (SST) images and climatological data. Stevenson (1977), combining *in situ* and SST satellite observations, identified an interesting thermal feature formed by a sequence of warm-cold-warm waters in NW-SE direction between Cadiz and Huelva

(the so called 'Huelva Front'). Fiúza (1983), using wind data and SST images corresponding to the summer of 1979, correlated the occurrence of upwelling off the southwest coast of Iberia (and the appearance of the Huelva Front) with westerlies and the development of a warm coastal countercurrent stretching east-west with easterlies (Fiúza et al., 1982, Fiúza, 1983). Folkard et al. (1997) analysed infrared SST satellite images throughout the year between July 1989 and March 1990 and reported a bimodal pattern in SST images related to wind regime in the summer months. Westerlies enhance the upwelling off CSV and promote its extension to the east. Additionally, a second core of upwelling appears off CSM that eventually merges with the one of CSV. Easterlies restricts the upwelling off CSV to a smaller area while, at the same time, a warm coastal countercurrent develops from east to west and displaces the upwelled waters offshore (García-Lafuente et al., 2006).

Relvas and Barton (2002) used a combined set of satellite data (1200 images between 1981 and 1995), coastal meteorological (wind, atmospheric pressure) and sea level observations at strategic points to study different areas of interest: the upwelling off the western Portuguese coast, the upwelling off the south coast of the Iberian Peninsula (Gulf of Cadiz), the filament off Cape St Vincent and the warm coastal countercurrent, all of them in relation to meteorological patterns. Sánchez and Relvas (2003) have analysed databases of hydrographic stations containing data for the whole 20<sup>th</sup> (1900-1998) corresponding to spring and summer on the southwest coast of the Iberian Peninsula and have depicted the climatic patterns of circulation in the Gulf of Cadiz during these seasons. The surface circulation in the Gulf of Cadiz is predominantly anticyclonic with some mesoscale meanders. Off Cape St Maria, the main current turns to the south and then to the north and continues flowing parallel to the Spanish coast. Finally, the branch that separates from the Strait of Gibraltar forms an anticyclonic meander in the easternmost region to feed the Canary Current (Sánchez and Relvas, 2003, Criado-Aldeanueva et al., 2006). This pattern is compatible with long currentmeter observations collected by the Red de Aguas Profundas (RAP) network of Puertos del Estado, Spain (see Figure 1 for location), although these records also report northwestwards velocities in wintertime. Some further research on wintertime circulation and its correlation with large scale and local wind forcing have been also recently accomplished by Sánchez et al. (2006).

Vargas et al. (2003), analysing a 8 year series of SST images have showed that the spatial pattern of the first empirical mode (which explains more than 60% of variance) indicates accumulation of warm light water in the middle of the basin, compatible with anticyclonic geostrophic circulation. But the time coefficients of the mode showed important seasonal variability with minimum values in winter which weaken the horizontal thermal gradient and may cause a reversal in the circulation during this season. Sub-surface temperature measurements taken *in situ* during previous surveys correlate reasonably well with satellite surface patterns and also show variability. Cruises carried out in 1995 and 1997 during the summer period showed different oceanographic patterns in the basin: in 1995, a pool of warm water near to the Guadalquivir River mouth was observed, whereas in 1997 a cold water front was registered in the same area (Rubín et al., 1997, 1999; García et al. 2002).

The GOLFO 2001 cruise provided a great amount of *in situ* data and more research has been recently carried out both on physical and biological topics. García-Lafuente et al. (2006) and Criado-Aldeanueva et al. (2006) depict the water mass circulation pattern on

the continental shelf and the outer region of the Gulf of Cadiz and describe some mesoscale features like the filament of CSM. The variability of the surface currents and geostrophic transports is discussed as well as some modifications in the continental shelf patterns due to wind induced variability (García-Lafuente et al., 2006) but, except for the continental shelf, no attention is paid to the variability of the 3-D thermohaline patterns and water masses distribution. Physical-biological coupling studies have identified different phytoplankton populations in connection with the variability in the water masses spatial distribution pattern (Reul et al., 2006, Navarro et al., 2006) and claim for further knowledge on this topic, to which is mainly devoted this paper.

The work is organised as follows: section 2 presents the data and methodology; section 3 discusses the variability observed both in the TS diagrams, in the 3-D fields and in the water masses distribution. To perform the latter, a technique based on the selection of three reference points in the TS diagram, is presented. Finally, section 4 summarises the conclusions.

## 2. DATA ACQUISITION AND METHODOLOGY

The interdisciplinary survey GOLFO 2001 was carried out in the waters of the Gulf of Cadiz between 14 May and 3 June 2001 onboard the oceanographic Research Vessel Hespérides, within the framework of the project MAR99-0643 ‘Distribution and Dynamics of Plankton and Seston in the Gulf of Cadiz: Variability Scales and Control by Physical and Biological Processes’. The survey was divided into three legs, called Mesoscale 1, Macroscale and Mesoscale 2, whose characteristics are summarised in Table 1 and whose geographical scope can be seen in Figure 1 (lower). More details of the station spacing, profiling time or data processing can be found in Criado-Aldeanueva (2004).

--- Approximate location of Table 1 ---

The data set includes hydrological data (Conductivity-Temperature-Depth, CTD Idronaut MK 137 with nephelometer and fluorometer SeaPoint and thermosalinographer SEABIRD SBE 21 for continuous recording of surface data), Acoustic Doppler Current Profiler (ADCP) velocity data (ADCP RDI VM150 –NB) and biological data (Rosette General Oceanics 1015 of 24 bottles). Additionally, air pressure and wind velocity was recorded by the RAP oceanographic buoy of the Gulf of Cadiz. Due to its offshore location, these data were considered as representative of the mean wind and pressure fields over the Gulf of Cadiz. Remote sensing SST data were obtained from the Deutsches Zentrum für Luft und Raumfahrt (DLR) through the public access gateway. Daily SST maps were composed using up to seven different NOAA satellite acquisitions through Advanced Very High Resolution Radiometers (AVHRR) onboard the NOAA. The spatial resolution is 1.1 km at the nadir. However, cloudy weather prevented the acquisition of good quality images during most of Mesoscale 1.

Following the directions of UNESCO (1985) the quantity  $\gamma_t$ , obtained from the temperature and salinity fields through the state equation, is used to express the density field. The use of  $\gamma_t$  instead of the potential density  $\gamma_\theta$  is appropriate due to the shallow depth (<1000m) of the sampled stations. The interpolation of the hydrological data has been carried out by means of the optimal or statistical interpolation technique, OI henceforth. This method, widely presented in the literature (Gandin, 1963; Thiébaux

and Pedder, 1987; Ruiz Valero, 2000; Gomis et al., 2001), is based on the condition that the differences between real field values and the results of the analysis are minimised statistically. The OI technique requires the adjustment of several parameters: for the tendency's *degree of the polynomial*, as low values are recommended (Thiebaut and Pedder, 1987),  $n = 2$  has been used. The *spatial scale correlation* has been established as 20 km, and the *noise-signal* ratio as 0.001 for CTD data (see Criado-Aldeanueva et al., 2006 for details). The same spatial grid step has been chosen for the three legs:  $0.1^\circ$  in coordinate  $x$  (longitude) and  $0.0548^\circ$  in coordinate  $y$  (latitude). The difference lies in the origin of the grid and, consequently, in the number of grid points. The values of these parameters for each leg are shown in Table 1.

### 3. RESULTS AND DISCUSSION

The wind regime drastically changed from westerlies during Mesoscale 1 and part of the Macroscale to easterlies during Mesoscale 2 (see Figure 2). This change has made it possible to study the response of the water masses distribution and 3D fields to this forcing. Due to its rather different wind regime, comparison will be mainly established between the two mesoscale samplings. In the Macroscale leg, widely discussed in Criado-Aldeanueva et al. (2006), westerlies were dominant but some of the oceanographic features related to this regime weaken and lead to those of easterlies. In this sense, it can be considered as a typical intermediate situation between the two mesoscales (Criado-Aldeanueva et al., 2006).

--- Approximate location of Figure 2 ---

#### 3.1 Variability of the TS diagrams

Strictly speaking, a water mass is defined by its temperature and salinity taken as conservative parameters only altered by mixing. Following this requirement, some of the water classes described below (SAW, SW) are not a water mass in strict sense, although, by extension, in some cases all of them will be referred as water masses in general. Fig 3 illustrates the TS diagrams obtained in the two mesoscale legs and different water masses were identified. Mainly, North Atlantic Central Water (NACW), characterised by a linear relation in the TS diagram ( $11.0^\circ\text{C} \leq T \leq 17.0^\circ\text{C}$ ;  $35.6 \leq S \leq 36.5$ ) and bounded by isopycnals  $26.6 \text{ kg}\cdot\text{m}^{-3} \leq \gamma_t \leq 27.3 \text{ kg}\cdot\text{m}^{-3}$ , was found in both cruises (see Figure 3). Below a certain depth, that is, from a certain isopycnal ( $27.1 \text{ kg}\cdot\text{m}^{-3} \leq \gamma_t \leq 27.3 \text{ kg}\cdot\text{m}^{-3}$  depending on the location), the TS diagram diverges from its former linear behaviour due to mixing with the underlying, salty Mediterranean Water (MW), that presents two main maxima in the TS diagram corresponding to the classical two cores (upper and lower) with different densities,  $\gamma_t \approx 27.5 \text{ kg}/\text{m}^3$  and  $\gamma_t \approx 27.8 \text{ kg}/\text{m}^3$  (see Figure 3), widely reported in the literature (Madelain, 1970; Zenk, 1970; Ambar and Howe, 1979a, b, Ambar et al., 2002). Comparison of Figures 3a and 3b evidences that the previous description is rather permanent within the two legs, thus showing (as expected) that NACW and MW are not sensitive to short time variations in the local wind regime.

--- Approximate location of Figure 3 ---

Air-sea interactions modify the upper layers of the water column and NACW becomes Surface Atlantic Water (SAW) characterised by  $T > 16.0^\circ\text{C}$ ,  $S \approx 36.4$  and  $\gamma_t \leq 26.7$

$\text{kg}\cdot\text{m}^{-3}$  (see Figure 3). Recently, Criado-Aldeanueva et al. (2006) have described Warm Shelf Waters (SW) over the eastern continental shelf. These waters are warmer and fresher than SAW and correspond to the points of the TS diagram with  $T > 16.0\text{ }^{\circ}\text{C}$  and  $35.9 \leq S \leq 36.5$  that are placed outside the line of NACW. Contrary to NACW and MW, SAW and SW suffer noticeably short-term, wind induced variability due to its shallower depth. According to García-Lafuente et al. (2006), the presence of localised spots of water warmer than the average requires the existence of a heat supply to maintain the surface thermal signature against heat advection and diffusion. Off Guadalquivir river mouth and Cadiz embayment, the heat source would be, apparently, the land. In this area,  $M_2$  amplitude is higher than 1m and the tide progresses inland through the different arms of the Guadalquivir river (similar happens in the neighbourhood of Cadiz embayment) flooding a few squared kilometres of marshes. Some concomitant mechanisms but, specially, the flooding of marshes that have been heated by sun radiation during the previous low tide lead to a greater absorption of energy per mass unit that is brought back to the sea during ebb tide (García Lafuente et al., 2006). The accumulation of warmer (and, hence, lighter) water in this part of the shelf creates an east to west along-shore sea surface slope that, if not baroclinically compensated, produces a pressure gradient in the interior. Westerlies (Mesoscale 1) increase this sea level slope as they pile up water against the coast but wind drag cancels the excess of sea level gradient force, thus preventing a surface counterflow to the west. This wind set up disappeared in Mesoscale 2 (under easterlies) and the warm water pool was no longer retained near Guadalquivir river mouth but it was released, invading the surface layer of the eastern (and partly western) continental shelf. Its fluvial influence would also explain the lower salinity of SW in comparison with SAW (García-Lafuente et al., 2006). For this reason, in Mesoscale 2, surface TS points have higher temperature than in Mesoscale 1 (compare  $T < 18^{\circ}\text{C}$  in Fig 3a with  $T$  above  $20^{\circ}\text{C}$  in Figure 3b) and most of them fall within the region of SW and SAW. Above  $\gamma_t \approx 27.0\text{ kg}\cdot\text{m}^{-3}$ , NACW suffers influence of SW. This fact along with reciprocal influence between SAW and SW confers the upper TS diagram a typical triangle shape that will be used in section 3.3 for further discussion.

### 3.2 Variability of the 3D fields

The temperature field at 10 m shows significant differences between Mesoscale 1 (Figure 4a) and Mesoscale 2 (Figure 4d). The mean temperature at this depth is more than  $3^{\circ}\text{C}$  lower in Mesoscale 1 (Table 2), sampled under westerlies. Additionally, NACW upwelled in Cape St Maria is clearly detected and it stretches eastwards from the Cape, giving rise to the surface thermal signature of the Huelva front and pushing to the east the pool of warmer water over the continental shelf (Figure 4a). On the contrary, in Mesoscale 2, accomplished under easterlies, upwelled waters have been confined to a smaller region west of Cape St Maria and pushed offshore to the south due to the spreading to the west of a SW coastal counter current (Figure 4d) that strengthens under easterlies (Fiúza et al., 1982; Fiúza, 1983; Folkard et al., 1997; Vargas et al., 2003; García-Lafuente et al., 2006). Macroscale leg (not shown) corresponds to an intermediate situation between the two mesoscales, although it is more similar to Mesoscale 1, as westerlies were dominant (Figure 2). Some of the features detected in Mesoscale 1 weaken (e.g., the upwelling off Cape St Maria) and those of Mesoscale 2 begin to appear (e.g., the development of the warmer coastal counter current).

--- Approximate location of Table 2 ---

Contrary to the temperature, salinity field at 10 m depth is rather uniform in both mesoscales (Figure 4b, e) and the value of the mean salinity is the same (Table 2). As previously shown, changes in wind regime promote heat inputs from land but, due to its land origin, no significant inputs of salty or fresh water are expected. Additionally, salinity of surface waters is rather similar to that of sub-surface ones (compare Figure 4b, e with Figure 5b, e), that is NACW becomes SAW or SW mainly by heating processes and salinity remains the same. In both legs, the surface signature of the filament of fresher water off Cape St Maria (see Criado-Aldeanueva et al., 2006) is clearly detected. Although the geographical scope of the samplings does not allow determining the position and dimension of the filament accurately, there are pieces of evidence that it could be slightly displaced to the west in Mesoscale 1. It might be that the wind induced variability of the geostrophic current that advects to the south the upwelled waters and gives rise to the filament (see Criado-Aldeanueva et al., 2006) promote some variations in its location.

--- Approximate location of Figure 4 ---

Due to the relatively slight spatial variation of the salinity field in relation to temperature, the density field is dominated by temperature. Thus, the variability observed in the temperature field at 10 m depth (Figure 4a, d) is also reflected in the density field at the same depth (see Figure 4c, f). The areas of cold upwelled NACW correspond with denser regions and those of warmer SAW correspond with less dense ones. Consequently, the maximum value of mean  $\gamma_t$  at 10 m is detected in Mesoscale 1 and the minimum in Mesoscale 2, being the difference about  $0.8 \text{ kg}\cdot\text{m}^{-3}$  (see Table 2).

At 50 m depth (Figure 5), the temperature field adopts a common pattern for both mesoscales, being the central warm core of SAW and the upwelled NACW over the whole continental shelf the most outstanding characteristics (Figure 5a, d). The mean temperature is rather similar for the two legs at this depth, less than  $1^\circ\text{C}$  higher in Mesoscale 2 (Table 2). The salinity field (Figure 5b, e) hardly shows response to the wind induced variability in the spatial patterns at 10 m depth and neither does it at 50 m. Saltier waters are located in the central warm core and fresher ones over the continental shelf. The density field (Figure 5c, f) is again dominated by temperature as it coincides denser waters with colder (although fresher) ones and less dense waters with warmer (although saltier) ones. Anyway, the spatial distribution of the density field is not sensitive to wind variations at this depth. Finally, at 100 m depth (not shown) the spatial distribution of the hydrological variables does not differ from the one described for 50 m and its mean values are almost the same for both legs (Table 2).

--- Approximate location of Figure 5 ---

The above description suggests that some hydrological surface patterns, particularly related to temperature and, hence, to density, are influenced by the wind regime. Wind changes produce great temporal variability in some spatial features (the upwelling off Cape Santa María, the surface signature of the Huelva Front, the region of warm coastal waters, etc) in a relatively shallow layer (<50 metres, see section 3.3 for details). Below this surface layer, the hydrological characteristics are fairly independent of meteorological forcing.

### 3.3 Variability of the surface water masses distribution

As previously shown, the short term, wind induced variability only affects some tens of meters of the water column. In this section, research on this variability is refined by studying the composition of the surface waters referred to three “standard” water classes defined in terms of the TS diagram.

#### *TS triangle in the surface layer*

Figure 6a, c emphasises the typical triangle shape of the upper layer of the TS diagram above  $\gamma_t \approx 27.0 \text{ kg}\cdot\text{m}^{-3}$ . Three apices have been selected for the triangle. Point A (green) corresponds to the TS properties of NACW located at  $\gamma_t \approx 27.0 \text{ kg}\cdot\text{m}^{-3}$ . Criado-Aldeanueva et al. (2006) show that this NACW suffers very little mixing and has well-defined temperature and salinity values ( $T \approx 13,2 \text{ }^\circ\text{C}$ ,  $S \approx 35,8$ ). Point B (blue) is located at the end of the linear TS relation of NACW and would correspond with the upper layer of NACW (that is, SAW) before being modified by air-sea interactions (mainly heating by radiation) that may raise its temperature. Finally, point C (red) is associated with SW and has been selected so that most of the TS points fall inside the triangle. As point C has not conservative TS properties, not only mixing processed but others like horizontal advection or air-sea exchanges may be involved. However, this selection has been proved to be useful to analyse the wind induced variability in the waters spatial distribution pattern. Not only physical properties of the water masses have been considered in the selection of the apices, but also biological ones. Reul et al. (2006) have identified different phytoplankton populations connected with the lines connecting each pair of apices and claim for further research on the physical underlying. The TS coordinates of the three apices are summarised in Table 3.

--- Approximate location of Table 3 ---

Once defined the three previous apices, temperature and salinity of any arbitrary point P of the TS diagram, can be expressed as a linear combination of temperature and salinity of the reference points A, B and C, that is:

$$T_p = a \cdot T_A + b \cdot T_B + c \cdot T_C \quad (1)$$

$$S_p = a \cdot S_A + b \cdot S_B + c \cdot S_C \quad (2)$$

where  $T_p$  and  $S_p$  are temperature and salinity of point P.  $T_A$ ,  $T_B$  and  $T_C$  are temperature of the reference points A, B and C and  $S_A$ ,  $S_B$  and  $S_C$  refer to salinity of the same three points. For the inner points (remind that the apices have been selected so that most of the TS points fall inside the triangle), the normalisation condition must stand:

$$a + b + c = 1 \quad (3)$$

Equations (1)-(3) can be solved for all the TS points of the TS diagram to obtain  $a$ ,  $b$  and  $c$ . Due to the existence of a set of values  $a$ ,  $b$  and  $c$  for any point P, the solution is dependent of the three spatial coordinates, thus providing spatial information on the water classes distribution. For practical purposes, the equations have been solved for vertical 5 meters averaged TS diagrams so that some spatial smoothing of the coefficients is achieved.

### *Water masses distribution in the surface layer*

Criado-Aldeanueva (2004) has performed a detailed analysis for 5 meters averaged TS diagrams concluding that the variability of the 3-D fields mainly affects the first 20-25 meters of the water column. Below this depth, proportion of water C is almost negligible everywhere and equation (3) is satisfied with the only contribution of coefficients  $a$  and  $b$  (corresponding to the “standard” waters A and B, respectively). Below 20-25m, water A is mainly located in the northern part of the Gulf, over the continental shelf, and water B occupies the central part of the Gulf, in good agreement with the description of section 3.2 for 50m depth. Much more interesting appears to be the discussion on water masses distribution based on the shallower 20m averaged TS diagrams, displayed in Figure 6b, d. Colours are in coherence with that assigned to the triangle apices (green for water A, blue for water B and red for water C).

--- Approximate location of Figure 6 ---

In Mesoscale 1 (Figure 6b), carried out under westerlies, high concentration (about 80%, see Figure 7a) of water A<sup>1</sup> is found in the northern part of the basin, also stretching to the east of the Cape Sta Maria, whereas the central part is filled with water B (above 80%, see Figure 7c), in good agreement with the description of section 3.2 for 10m depth. Water C is scarcely found (under 20%, Figure 7e) except in the northwestern part of the sampling region (about 20-30%, see Figure 7e again), in coherence with the few TS points that separate from the NACW line in the TS diagram (see Figure 3a). This distribution does not differ significantly from that of 50m depth, except for the traces of water C in the northwestern region. In Mesoscale 2, accomplished under easterlies, things are completely different. Water B is again located in the central part of the Gulf, but is modified by the presence of water C (compare the bright blue tones of Figure 6b with the ones of Figure 6d). Water A is restricted to a smaller region west of Cape Sta Maria and also suffers the influence of water C (percentage of water A in Figure 7b, about 60%, is lower than in Figure 7a). Precisely, water C is the most abundant (above 70% in the northwestern region) in this shallower layer (see also the TS diagram, Figure 3b), as it floods almost the whole continental shelf from Cadiz to west of Cape Sta Maria advected by the coastal countercurrent that strengthens under this wind regime (Fiúza et al., 1982; Fiúza, 1983; Folkard et al., 1997; Vargas et al., 2003; García-Lafuente et al., 2006). The above description confirms the wind induced variability depicted in section 3.2 and restricts its influence to a relatively shallow layer (20-25m). As previously pointed, Macroscale shares features of both mesoscales, mainly that of Mesoscale 1 as westerlies were dominant, and could be considered as an intermediate (averaged) situation between the two mesoscales.

--- Approximate location of Figure 7 ---

## **4. CONCLUSIONS**

From the data collected during GOLFO 2001 survey, a study has been conducted on the distribution of water masses in the Gulf of Cadiz in the spring of 2001, and on its meteorologically forced variability. In Mesoscale 1, westerlies were dominant while Mesoscale 2 was a period of strong easterlies. This variability has made it possible to

---

<sup>1</sup> Water A (B, C) in the following discussion really means water with TS properties similar to those of “standard” water A (B, C).

study the response of the oceanographic features to meteorological forcing using *in situ* data. The temperature field at 10 m shows significant differences between Mesoscale 1 and Mesoscale 2, the mean temperature at this depth being more than 3°C lower in Mesoscale 1. During this leg, NACW upwelled in Cape St Maria is detected stretching eastwards from the Cape, leaving a clear surface thermal signature of the Huelva front and pushing the pool of warmer water over the continental shelf to the east. On the contrary, in Mesoscale 2, upwelled waters were confined to a smaller region west of Cape St Maria and pushed offshore to the south due to the spreading of the warm SW to the west advected by the coastal counter current.

This variability also reflects in the upper layer of the TS diagrams. Reciprocal influence between NACW and SW and between SAW and SW confer this upper layer a typical triangle shape, in which three “standard” TS apices have been selected. Point A corresponds to the TS properties of NACW at  $\gamma_t \approx 27.0 \text{ kg}\cdot\text{m}^{-3}$ , point B corresponds to SAW before being modified by air-sea interactions and point C is associated with SW and has been selected so that most of the TS points fall inside the triangle. Considering the shallower 20m averaged TS diagrams, in which most of the variability is concentrated, some remarks are of concern: in Mesoscale 1, high concentration of water A is found in the northern basin, also stretching to the east of Cape Sta Maria, whereas water B fills the central basin. Water C is scarcely found except in the northwestern part of the sampling region. In Mesoscale 2, water B is again located in the central part of the Gulf, but noticeably modified by the presence of water C. Water A is restricted to a smaller region west of Cape Sta Maria and is also influenced by water C, the most abundant in this shallower layer, as it floods almost the whole continental shelf from Cadiz to west of Cape Sta Maria advected by the coastal countercurrent that develops under easterlies.

## ACKNOWLEDGEMENTS

We would like to thank the UIB-IMEDEA (Special Action CICYT, REN2000-2599-E) for the dissemination of the software used for the optimal interpolation. Wind data from the RAP buoy has been kindly yield by Puertos del Estado. We are also indebted to the crew of BIO Hespérides for his work during GOLFO 2001 survey. F. Criado Aldeanueva is much obliged to the Spanish Ministry of Education and Science for awarding him a F.P.U. grant (reference n°. AP2000-3951).

## REFERENCES

- Alves, M., Gaillard, F., Sparrow, M., Knoll, M. and Giraud, S. (2002). Circulation patterns and transport of the Azores front – current system. *Deep-Sea Res. II* 49, 3983-4002.
- Ambar, I. and Howe, M.R. (1979a). Observations of the Mediterranean outflow I: mixing in the Mediterranean outflow. *Deep-Sea Res.*, 26A, 535-554.
- Ambar, I. and Howe, M.R. (1979b). Observations of the Mediterranean outflow II: the deep circulation in the vicinity of the Gulf of Cadiz. *Deep-Sea Res.*, 26A, 555-568.
- Ambar, I., Serra, N., Brogueira, M.J., Cabeçadas, G., Abrantes, F., Freitas, P., Gonçalves, C. and Gonzalez, N. (2002). Physical, chemical and sedimentological aspects of the Mediterranean outflow Off Iberia. *Deep-Sea Research II* 49, 4163-4177.

Baringer, M.O. and Price, J.F. (1999). A review of the physical oceanography of the Mediterranean outflow. *Marine Geology* 155, 63-82.

Bryden, H.L. and Stommel, H.M. (1982). Origin of the Mediterranean outflow. *Journal of Marine Research* 40, 55-71.

Criado-Aldeanueva, F. (2004, in Spanish). Distribución y circulación de masas de agua en el Golfo de Cádiz. Variabilidad inducida por el forzamiento meteorológico. PhD, University of Málaga. ISBN: 84-689-0245-4. Published by the Publication Service University of Málaga.

Criado-Aldeanueva, F., García-Lafuente, J., Vargas, J.M., Del Río, J., Vázquez, A., Reul, A. and Sánchez, A. (2006). Distribution and circulation of water masses in the Gulf of Cadiz from *in situ* observations. *Deep-Sea Research II* (in press).

Fiúza, A.F.G., de Macedo, M.E. and Guerreiro, M.R. (1982). Climatological space and time variations of the Portuguese coastal upwelling. *Oceanol. Acta* 5, 31-40.

Fiúza, A.F.G. (1983). Upwelling patterns off Portugal. In: Suess, E., Thiede, J. (eds), *Coastal Upwelling*. Plenum, New York, 85-98.

Folkard, A.M., Davies, P.A., Fiúza, A.F.G. and Ambar, I. (1997). Remotely sensed sea surface thermal patterns in the Gulf of Cadiz and Strait of Gibraltar: variability, correlations and relationships with the surface wind field. *J. Geophys. Res.* 102, 5669-5683.

Gandin, L. (1963). Objective analysis of meteorological fields. Transl. from Russian by Israel Program for Scientific Translations, 1965 (NTIS N°. TT65-50007).

García, C.M., Prieto, L., Vargas, M., Echevarría, F., García Lafuente, J., Ruiz, J. and Rubín, P. (2002). Hydrodynamics and the spatial distribution of plankton and TEP in the Gulf of Cádiz (SW Iberian Peninsula). *Journal of Plankton Research*, 24 n°8, 817-833.

García-Lafuente, J., Delgado, J., Criado-Aldeanueva, F., Bruno, M., Del Río, J., Vargas, J.M. (2006). Water mass circulation on the continental shelf of the Gulf of Cadiz. *Deep-Sea Research II* (in press).

Gomis, D., Ruiz, S. and Pedder, M.A. (2001). Diagnostic analysis of the 3D ageostrophic circulation from a multivariate analysis of CTD and ADCP data. *Deep-Sea Res.* I, 48/1, 269-295.

Madelain, F. (1970, in French). Influence de la topographie du fond sur l'écoulement Méditerranéen entre le Détroit de Gibraltar et le Cap Saint -Vincent. *Cahiers Océanographiques* 22, 43-61.

Navarro, G., Ruiz, J., García, C.M., Criado-Aldeanueva, F. and Echevarría, F. (2006). Basin scale structures governing the position of the deep fluorescence maximum in the Gulf of Cádiz. *Deep-Sea Research II* (in press).

Ochoa, J. and Bray, N.A. (1991). Water masses exchange in the Gulf of Cadiz. *Deep-Sea Research* 38 Suppl.1, S465-S503.

Relvas, P. and Barton, E.D. (2002). Mesoscale patterns in the Cape Sao Vicente (Iberian Peninsula) upwelling region. *Journal of Geophysical Research*, 107(C10), 3164-3186.

Reul, A., Muñoz, M., Criado-Aldeanueva, F. and Rodríguez, V. (2006). Spatial distribution of phytoplankton < 13µm in the Gulf of Cadiz in relation to water masses and circulation pattern under westerly and easterly wind regimes. *Deep-Sea Research II* (in press).

Rubín, J.P., Cano, N., Arrate, P., García Lafuente, J., Escáñez, J., Vargas, M., Alonso Santos, J.C. and Hernández, F. (1997, in Spanish). El ictioplancton, el mesozooplancton y la hidrología en el Golfo de Cádiz, Estrecho de Gibraltar y sector noroeste del Mar de Alborán en Julio de 1994. *Inf. Téc. Inst. Esp. Oceanogr.*, 167, 44pp.

Rubín, J.P., Cano, N., Prieto, L, García, C.M., Ruiz, J., Echevarría, F., Corzo, A., Gálvez, J.A., Lozano, F., Alonso Santos, J.C., Escánez, J., Juárez, A., Zabala, L., Hernández, F., García Lafuente, J. and Vargas, M. (1999, in Spanish). La estructura del ecosistema pelágico en relación con las condiciones oceanográficas y topográficas en el Golfo de Cádiz, Estrecho de Gibraltar y Mar de Alborán (sector noroeste) en Julio de 1995. *Inf. Téc. Inst. Esp. Oceanogr.*,175, 73pp.

Ruiz Valero, S. (2000, in Spanish). Análisis espacial objetivo de datos oceanográficos: aplicaciones en el Mar de Alborán. PhD, University of Islas Baleares-IMEDEA.

Sánchez, R. and Relvas, P. (2003). Spring – summer climatological circulation in the upper layer in the region of Cape St. Vincent, southwest Portugal. *ICES Journal of Marine Science*, 60, 1232-1250.

Sánchez, R., Mason, E., Relvas, P., da Silva, A.J. and Peliz, A.J. (2006). On the inshore circulation in the northern Gulf of Cádiz, southern Portuguese shelf. *Deep-Sea Research II* (in press).

Serra, N. and Ambar, I. (2002). Eddy generation in the Mediterranean undercurrent. *Deep-Sea Research II*, 49, 4225-4243.

Stevenson, R.E. (1977). Huelva Front and Malaga, Spain, Eddy Chain as Defined by Satellite and Oceanographic Data. *Dtsch. Hydrogr. Z.* 30(2), 51-53.

Thiébaux, H.J. and Pedder, M.A. (1987). Spatial objective analysis with applications in atmospheric sciences. Academic Press, 299 pp.

UNESCO (1985). The International system of units in Oceanography. UNESCO Technical Paper n°. 45, Paris. United Nations Educational, Scientific and Cultural Organization.

Vargas, J.M., García-Lafuente, J., Delgado, J. and Criado, F. (2003). Seasonal and wind-induced variability of sea surface temperature patterns in the Gulf of Cádiz. *Journal of Marine Systems* 38, 205-219.

Zenk, W. (1970). On the temperature and salinity structure of the Mediterranean water in the northeast Atlantic. *Deep-Sea Research* 17, 627-631.

Zenk, W. and Armi, L. (1990). The complex spreading pattern of Mediterranean water off the Portuguese continental slope. *Deep-Sea Res., Part A*, 37, 1805-1823.

## FIGURE CAPTIONS

**Table 1:** Characteristics of the three legs of the GOLFO 2001 survey. Inclination refers to the angle of deviation from the meridians. The last two rows are related to the optimal interpolation technique parameters (see section 2).

**Table 2:** Mean values of temperature, salinity and density fields at 10m, 50 and 100m depth for the two mesoscale legs. Mean temperature at 10m depth is more than 3°C lower in Mesoscale 1 and hence, mean density at this depth is higher in this leg. Both at 50m and 100m depth the mean values in both legs are rather similar for the three variables.

**Table 3:** TS coordinates of the three apices selected for the triangle shape of the upper Ts diagrams (see also Figure 6). The criteria used for this selection are discussed in section 3.3.

**Figure 1:** Upper panel: Map of the Gulf of Cadiz showing the position of locations and other geographical features mentioned in the text. CT, CSM and CSV stand for Cape Trafalgar, Cape St. Maria and Cape St. Vincent, respectively. Grm, Orm, Trm and Gqrm stand for the mouths of Guadiana, Odiel, Tinto and Guadalquivir rivers, respectively. The star marks the position of the Red de Aguas Profundas (RAP) oceanographic buoy mentioned in the text. Lower panels show the station grid of the Mesoscale 1 and Mesoscale 2 legs of GOLFO 2001 survey.

**Figure 2:** Stick diagram of the wind regime from the RAP buoy (see Figure 1 for location) during May-June 2001. Time period of each survey has been indicated. Westerlies prevailed during Mesoscale 1 and the previous days; Macroscale was sampled under both regimes although westerlies were more frequent and intense. Mesoscale 2 was influenced by the moderate to strong and rather persistent episode of easterlies.

**Figure 3:** Temperature-Salinity (TS) diagrams of all the stations of Mesoscale 1 (panel a) and Mesoscale 2 (panel b) legs during GOLFO 2001 survey. NACW, SAW, SW and MW are the acronyms for North Atlantic Central Water, Surface Atlantic Water, Shelf Water and Mediterranean Water, respectively. The labels are roughly located at the theoretical positions of these water masses on the TS diagram. Some  $\gamma_t$  isopycnals have been superimposed for clarity.

**Figure 4:** Temperature (°C, panels a, d), salinity (panels b, e) and density ( $\gamma_t$ , kg·m<sup>-3</sup>, panels c, f) at 10m depth from Mesoscale 1 (upper panels) and Mesoscale 2 (lower panels) data. Notice the high variability detected both in the temperature and density fields.

**Figure 5:** Temperature (°C, panels a, d), salinity (panels b, e) and density ( $\gamma_t$ , kg·m<sup>-3</sup>, panels c, f) at 50m depth from Mesoscale 1 (upper panels) and Mesoscale 2 (lower panels) data. Stations shallower than 50m have been blanked. Surface horizontal variability shown in Figure 4 is no longer detected at this depth.

**Figure 6:** Detail of the upper layer of the TS diagrams for Mesoscale 1 (panel a) and Mesoscale 2 (panel c). The triangle shape characteristic of this upper layer has been

emphasised by drawing the lines between the three apices selected (see Table 3 for the coordinates). The criteria used for this selection are discussed in section 3.3. The colour code for each apex is in connection with the averaged upper 20m spatial distribution showed in the right panels for Mesoscale 1 (panel b) and Mesoscale 2 (panel d). Notice that in Mesoscale 1 (under westerlies), the balance is almost established between waters A and B whereas in Mesoscale 2 (under easterlies), high concentration of water C is detected in the northern and eastern continental shelf, thus showing the wind induced variability that affects the surface layer. Further details are discussed in the text.

**Figure 7:** Spatial distribution pattern of the percentages (expressed in %) of the three “standard” water types A (panels a, b), B (panels c, d) and C (panels e, f) for the upper 20m water column in Mesoscales 1 (left panels) and 2 (right panels). Calculations have been carried out from equations (1)-(3). The wind induced variability of the waters spatial distribution is revealed. In Mesoscale 1 (under westerlies), the balance is almost established between waters A and B whereas in Mesoscale 2 (under easterlies), high percentage of water C is detected in the northern and eastern continental shelf.

## TABLES

	Mesoscale 1	Macroscale	Mesoscale 2
Sample dates	14/05/01 – 16/05/01	17/05/01 – 24/05/01	29/05/01 – 02/06/01
N° of transects	7	12	11
Longitude range	6.92°W - 8.18°W	6.27°W – 9.28°W	6.51°W – 8.59°W
Latitude range	36.58°N – 37.08°N	36.01°N – 37.13°N	36.57°N – 37.08°N
Inclination	-	15°	-
Origin coordinates	(8.30°W-36.54°N)	(9.20°W-36.00°N)	(8.70°W-36.54°N)
Number of points	12 x 15	22 x 31	12 x 23

Table 1: Characteristics of the three legs of the GOLFO 2001 survey. Inclination refers to the angle of deviation from the meridians. The last two rows are related to the optimal interpolation technique parameters (see section 2).

<b>Leg</b>	<b>Variable</b>	<b>10 m</b>	<b>50 m</b>	<b>100 m</b>
<b>Mesoscale 1</b>	<b>Temperature (°C)</b>	<b>15,57 ± 0,38</b>	15,12 ± 0,87	14,76 ± 0,42
	<b>Salinity</b>	36,00 ± 0,05	36,10 ± 0,09	36,01 ± 0,08
	<b>Gamma-t (kg/m<sup>3</sup>)</b>	26,60 ± 0,09	26,77 ± 0,08	26,84 ± 0,03
<b>Mesoscale 2</b>	<b>Temperatura (°C)</b>	<b>19,04 ± 0.71</b>	15,72 ± 0,33	15,08 ± 0,21
	<b>Salinity</b>	36,01 ± 0,09	36,14 ± 0,08	36,11 ± 0,04
	<b>Gamma-t (kg/m<sup>3</sup>)</b>	25,81 ± 0,09	26,68 ± 0,04	26,80 ± 0,02

Table 2: Mean values of temperature, salinity and density fields at 10m, 50 and 100m depth for the two mesoscale legs. Mean temperature at 10m depth is more than 3°C lower in Mesoscale 1 and hence, mean density at this depth is higher in this leg. Both at 50m and 100m depth the mean values in both legs are rather similar for the three variables.

<b>Apex</b>	<b>Temperature (°C)</b>	<b>Salinity</b>
A	13.20	35.80
B	17.50	36.55
C	21.30	35.97

Table 3: TS coordinates of the three apices selected for the triangle shape of the upper Ts diagrams (see also Figure 6). The criteria used for this selection are discussed in section 3.3.

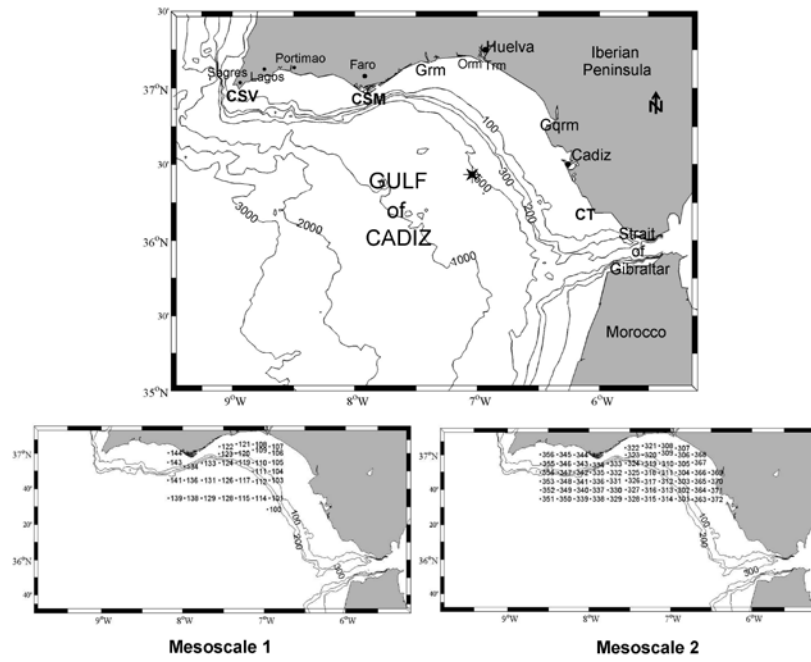


Figure 1

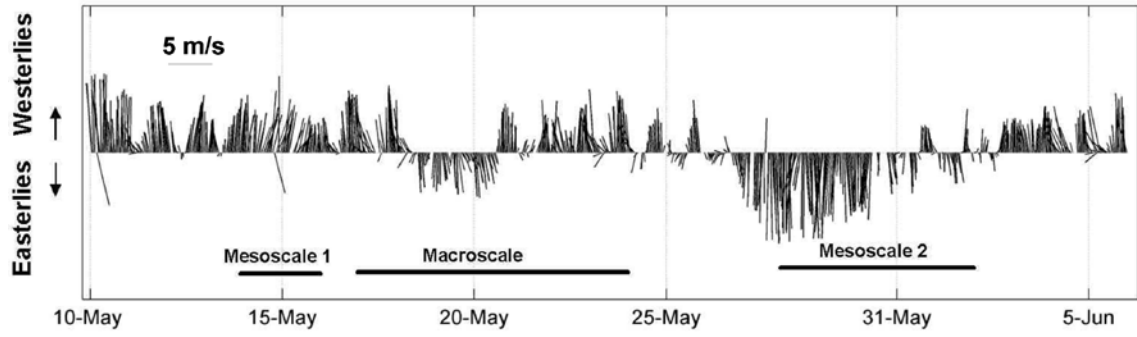


Figure 2

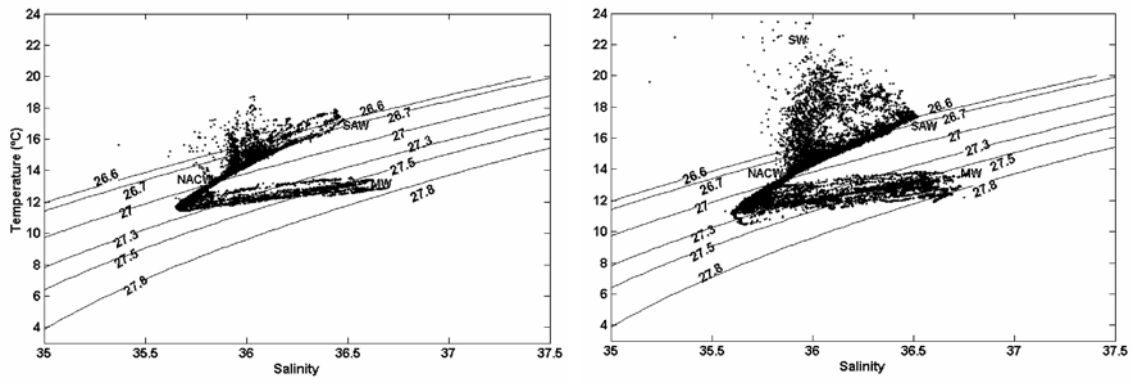


Figure 3

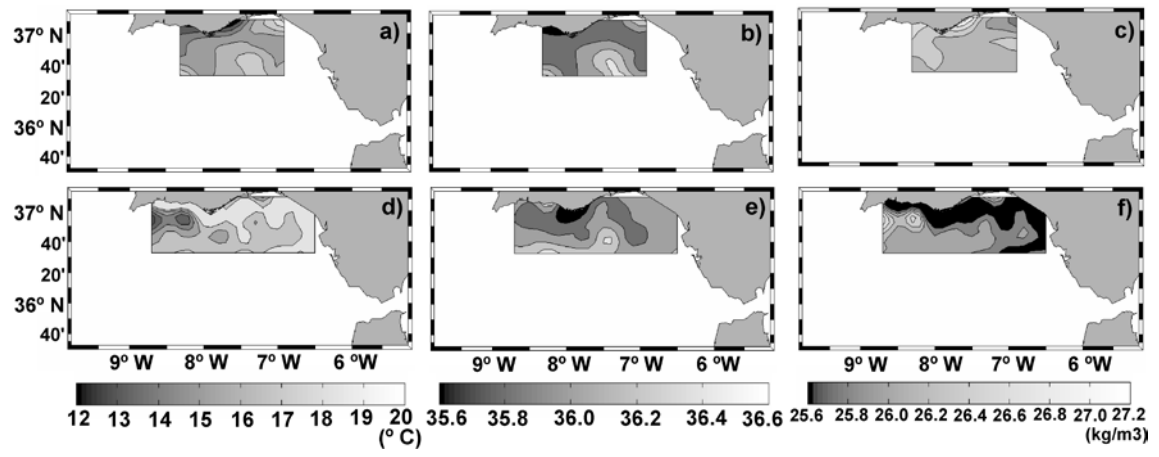


Figure 4

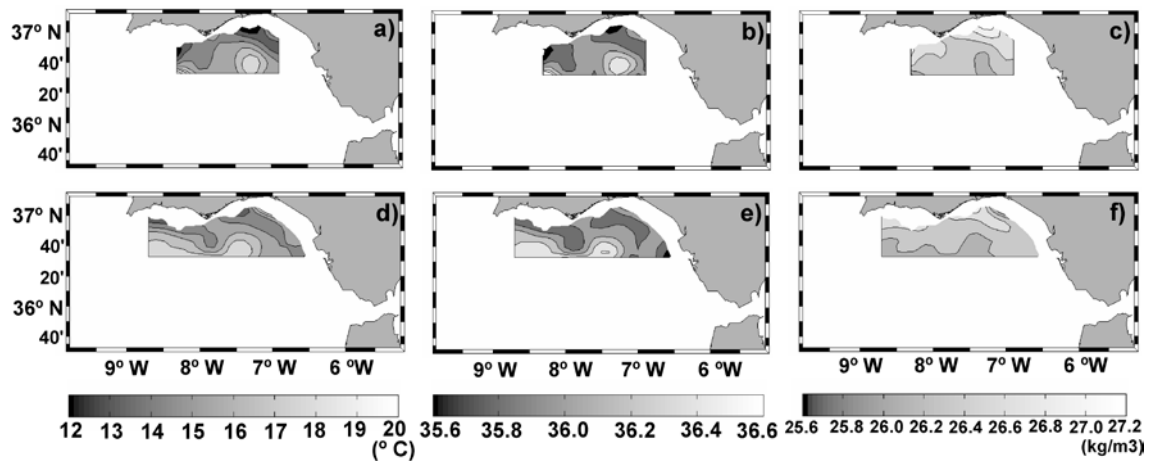


Figure 5

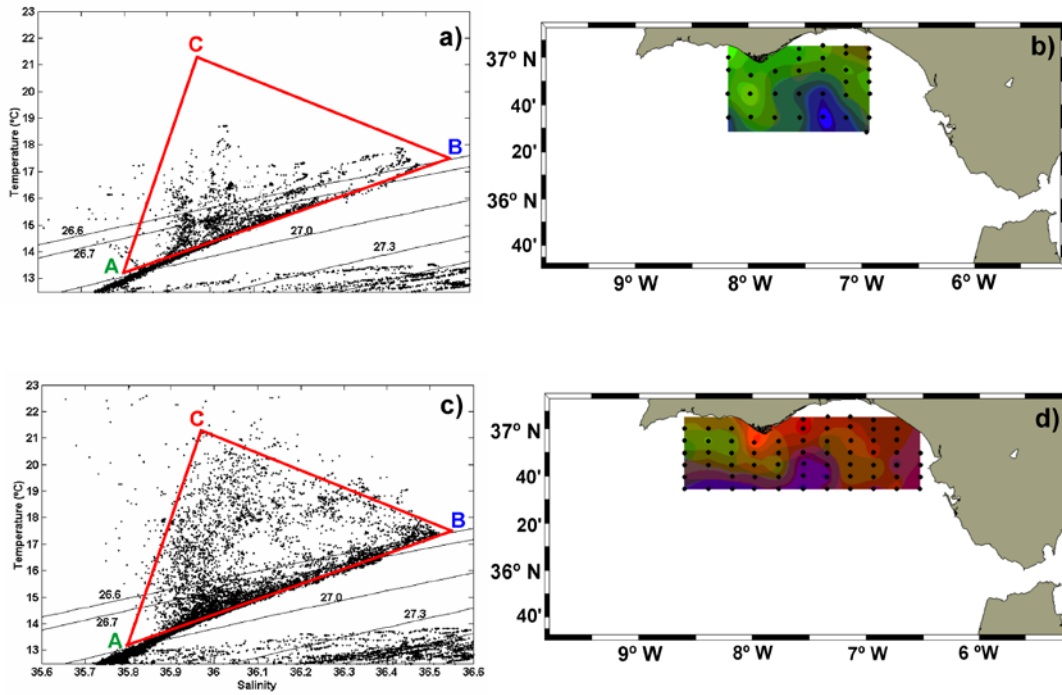


Figure 6

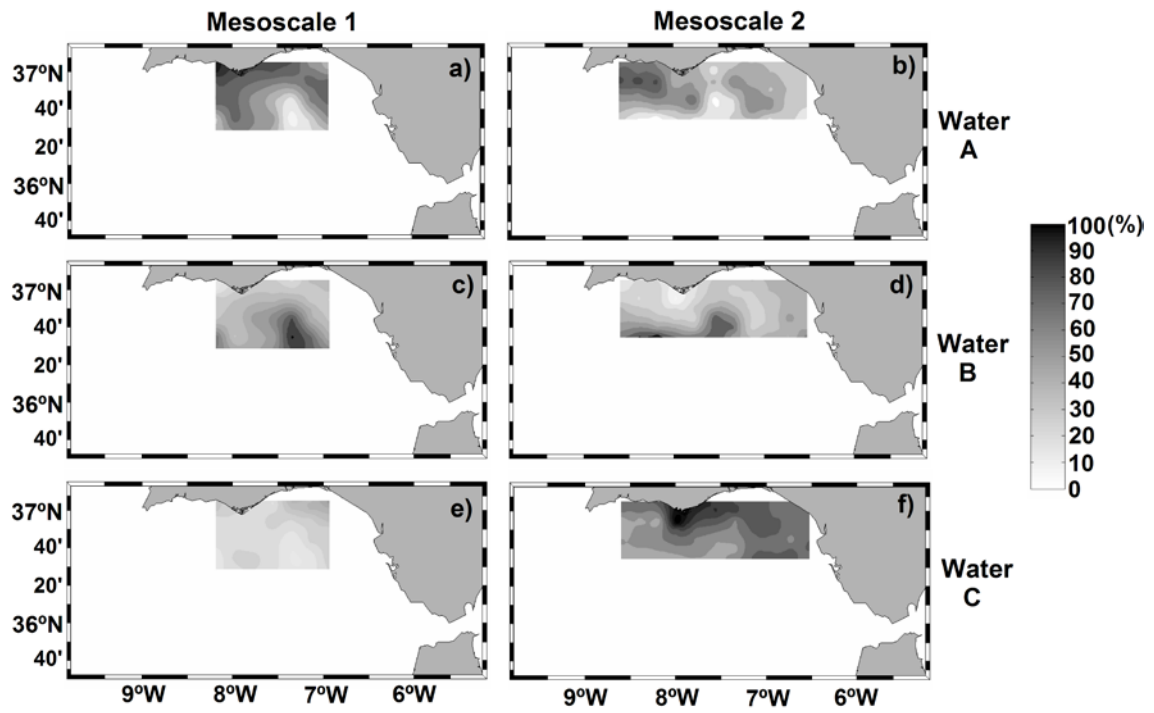


Figure 7